JOURNAL OF
Materials
CHEMISTRY

Photocurrent generation using gold electrodes modified with self-assembled monolayers of a fullerene–porphyrin dyad

Hiroko Yamada,[a] Hiroshi Imahori*[a,b] and Shunichi Fukuzumi*[a]

[a] *Department of Material and Life Science, Graduate School of Engineering, Osaka University, CREST, JAPAN Science and Technology Corporation (JST), Suita, Osaka, 565-0871, Japan. E-mail: imahori@mee3.moleng.kyoto-u.ac.jp; fukuzumi@chem.eng.osaka-u.ac.jp*
[b] *Department of Molecular Engineering, Graduate School of Engineering, Kyoto University, PRESTO, Sakyo-ku, Kyoto 606-8501, Japan*

Received 10th January 2002, Accepted 6th March 2002
First published as an Advance Article on the web 3rd April 2002

Self-assembled monolayers (SAMs) of a fullerene–porphyrin linked dyad and a porphyrin reference on a gold electrode have been prepared to exhibit anodic photocurrent generation instead of cathodic photocurrent generation for the first time. The spectroscopic and electrochemical studies reveal the densely-packed structure of the fullerene–porphyrin dyad on the gold electrode. The photoelectrochemical properties of SAMs of the fullerene–porphyrin dyad in the presence of an electron donor were examined and compared with those of the porphyrin reference without the fullerene otherwise under the same conditions. The quantum yield of photocurrent generation for the fullerene–porphyrin dyad cell is much larger than that of the porphyrin reference. These results clearly demonstrate that C_{60} is a good electron mediator between the porphyrin moiety and the gold electrode.

Introduction

Self-assembled monolayers (SAMs) have recently attracted much interest towards advancement of nanotechnology,[1] since they can provide densely packed, well-ordered architecture on metal or semiconductor surfaces. In particular, alkanethiols on gold surfaces have been the most well-studied systems because of their relatively easy accessibility. Functionalization on the gold surfaces has been achieved by incorporating electro- and photo-active chromophores such as fullerenes,[2–4] porphyrins,[5–8] and others[9–12] at the end of alkanethiols or equivalents. In this context, SAMs of single photoactive chromophores on flat gold surfaces[4,8] have been developed as photovoltaic devices to exhibit photocurrent generation. However, inefficient electronic interaction between the chromophore and the gold electrode has precluded achievement of a high quantum yield for photocurrent generation on gold surfaces. Such lack of communication between the chromophore and the gold electrode can be surmounted when an electron mediator has been introduced between the photoactive chromophore and the gold electrode. Electron mediators such as ferrocene,[5c] quinone,[5d] and viologen[5a,b,11e] have so far been used in such systems to achieve highly efficient multistep electron transfer (ET) by mimicking photosynthetic ET on gold electrodes.

Porphyrins and fullerenes have frequently been employed as an electron donor and an electron acceptor, respectively, in donor–acceptor linked systems.[13,14] We have demonstrated that fullerenes have small reorganization energies of ET, which lead to remarkable acceleration of photoinduced CS and of charge shift (CSH) and retardation of charge recombination (CR), as compared to conventional acceptors (*i.e.*, quinones).[15,16] Thus, a number of porphyrin–fullerene linked systems have been prepared to generate a long-lived charge-separated state with a high quantum yield *via* photoinduced ET in solutions.[17] Such porphyrin–fullerene linked molecules have been successfully incorporated into SAMs on gold electrodes to reveal cathodic photocurrent generation.[18] However, alternative anodic photocurrent generation has yet to be reported in SAMs of porphyrin–fullerene linked systems on gold electrodes because of the synthetic difficulties.

We report herein the construction of SAMs of fullerene–porphyrin dyads on Au(111) (denoted as **C_{60}–H_2P/Au** in Fig. 1) to achieve anodic photocurrent generation. The porphyrin and the C_{60} moieties and the C_{60} and the disulfide moieties are linked *via* long alkyl spacers. Thus, the fullerene–porphyrin linked molecules (**C_{60}–H_2P** in Fig. 1) are expected to be well-packed on the gold electrodes where the components of **C_{60}–H_2P** are arranged in the order: the gold electrode, the C_{60}, and the porphyrin, as in the case of alkanethiols on gold surfaces. The resulting structure of **C_{60}–H_2P/Au** was characterized using UV-visible absorption spectroscopy and cyclic voltammetry. The photoelectrochemical properties were also examined in the presence of an electron donor [*i.e.*, triethanolamine (TEA), ascorbic acid (AsA), and ethylenediaminetetraacetic acid (EDTA)] in the electrolyte solution and they are compared to those of the reference porphyrin SAM (denoted as **H_2P/Au** in Fig. 1)[8c] without C_{60}.

Results and discussion

Preparation of SAMs

The preparation of **C_{60}–H_2P** was carried out as shown in Scheme 1. Porphyrin **1** was prepared by condensation of pyrrole with 3,5-di-*tert*-butylbenzaldehyde[19] and 4-hydroxybenzaldehyde in propionic acid.[20] Hydroxyporphyrin **1** was linked to 1,11-dibromoundecane, 3,5-dihydroxybenzaldehyde, and 1,12-dibromododecane, successively, to give bromoporphyrin **4** *via* **2** and **3**. Bromide **4** was converted to disulfide **6** *via* nucleophilic substitution with potassium thioacetate and subsequent base deprotection of **5**. Porphyrin dimer **6** underwent 1,3-dipolar cycloaddition with C_{60} using *N*-methylglycine to give **C_{60}–H_2P**.[21] The porphyrin reference (**H_2P**) was prepared by following the same procedure as described previously (Fig. 1).[17b] Their structures were verified by spectroscopic analyses (see Experimental section).

The **C_{60}–H_2P** was self-assembled on Au(111) as follows.[8c] The gold electrodes with an Au(111) surface were dipped into a CH_2Cl_2 solution of **C_{60}–H_2P** at 25 °C for 20 h under an argon atmosphere. After completing the modification, **C_{60}–H_2P/Au** was rinsed copiously with CH_2Cl_2 and EtOH and dried with a

DOI: 10.1039/b200379a

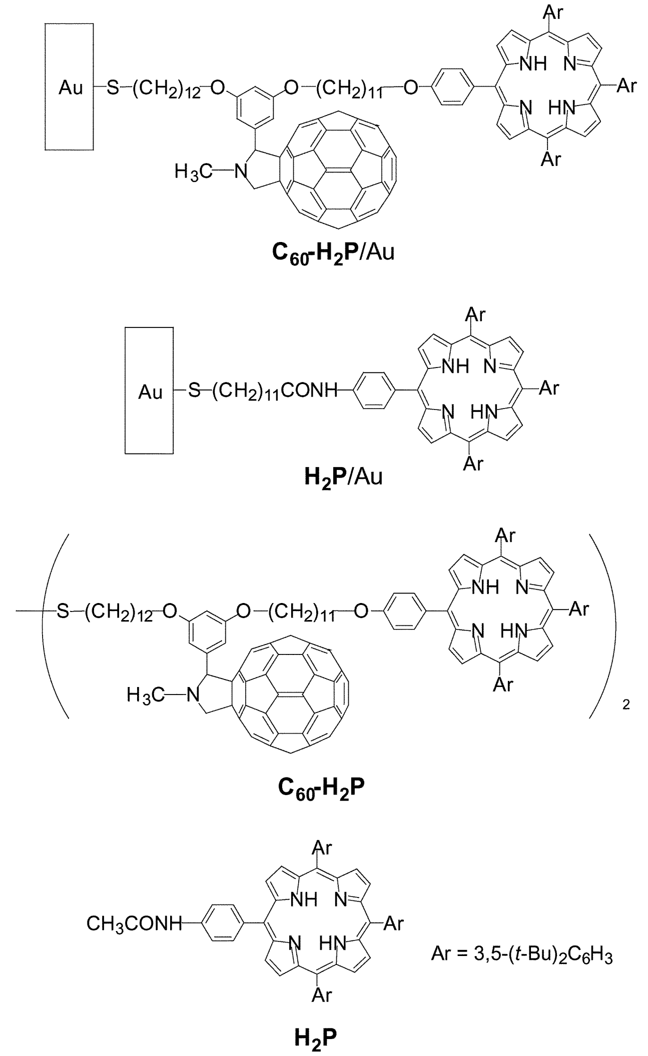

Fig. 1 Self-assembled monolayers of the fullerene–porphyrin dyad and porphyrin on gold electrodes and their reference compounds.

stream of nitrogen. **H_2P**/Au as a reference was also prepared by following the same procedure as described for **C_{60}–H_2P**/Au.[8c]

Absorption spectroscopy

Fig. 2a displays the absorption spectra of **C_{60}–H_2P**/Au and the reference **C_{60}–H_2P** in THF. The Soret band of **C_{60}–H_2P**/Au becomes broader than that of **C_{60}–H_2P** in THF. The $\lambda_{\max}$ value of the Soret band of **C_{60}–H_2P**/Au (426 nm) is red-shifted by 6 nm as compared to that of **C_{60}–H_2P** in THF (420 nm). In the case of **H_2P**/Au, the porphyrin moieties are reported to be densely packed on Au(111).[8c] A similar red-shift (8 nm) was noted for the $\lambda_{\max}$ value of **H_2P**/Au (428 nm)[8c] relative to that of reference **H_2P** in THF (420 nm).[22] This indicates that the porphyrin environments of **C_{60}–H_2P**/Au and **H_2P**/Au are virtually the same and perturbed significantly within the monolayers, as compared to the references in THF, due to the porphyrin aggregation.[8c]

Cyclic voltammetry

The cyclic voltammetric measurements of **C_{60}–H_2P**/Au (Fig. 3a) and **C_{60}–H_2P** (Fig. 3b) in CH_2Cl_2 containing 0.2 M n-Bu_4NPF_6 were performed with a sweep rate of 0.10 V s^{-1} (electrode area, 0.48 cm^{-2}) to estimate the surface coverage. In the case of **C_{60}–H_2P** in CH_2Cl_2, three successive waves due to the reduction of the C_{60} moiety [−0.78, −1.20, and −1.56 V *vs.* Ag/AgCl (sat. KCl)] and a wave due to the first oxidation of the porphyrin [E^0_{ox} = 0.97 V *vs.* Ag/AgCl (sat. KCl)] were observed, whereas the second wave due to the second oxidation of the porphyrin was irreversible, as shown in Fig. 3b. The cyclic voltammogram of **C_{60}–H_2P**/Au (Fig. 3a) is characterized by a couple of reversible waves due to the first oxidation of the porphyrin and an irreversible wave due to the second oxidation of the porphyrin. The first anodic current increased linearly when increasing the scan rate, implying that the porphyrin is a surface-confined electroactive molecule. The E^0_{ox} value [1.05 V *vs.* Ag/AgCl (sat. KCl)] was determined as the average of the anodic and cathodic peak potentials. The first E^0_{ox} of **C_{60}–H_2P**/Au is shifted to the positive direction (80 mV) as compared to that of **C_{60}–H_2P** in CH_2Cl_2. The positive shift of E^0_{ox} in the SAM may result from the decreased dielectric constant in the nonpolar monolayer as compared to that of the bulk solution.[8c] On the other hand, the electrochemical response due to the C_{60} moiety was not reversible for **C_{60}–H_2P**/Au. Similar behavior was reported for ferrocene–porphyrin–C_{60} SAMs on gold electrodes.[18c] Such irreversible behavior due to the reduction of the C_{60} moiety can be rationalized by the electrochemical inaccessibility of the C_{60} moiety which is deeply buried into the SAM.

The adsorbed amounts (Γ) of the compound on **C_{60}–H_2P**/Au were calculated to be 1.9 (±0.2) × 10^{-10} mol cm^{-2} (87 (±8) Å^2 molecule^{-1}) by dividing the first anodic peak currents of the porphyrin (9.7 ± 0.9 μC cm^{-2}) by the Faraday constant and the roughness factor = 1.1.[8c] The value is comparable to the adsorbed amounts of ferrocene–porphyrin–C_{60} triad SAM (1.9 × 10^{-10} mol cm^{-2}),[18c] where the triad molecules are well-packed with an almost perpendicular orientation on the gold surface.[23] Thus, we can conclude that **C_{60}–H_2P** molecules are densely packed on the gold surface in the order: the gold surface, the C_{60}, and the porphyrin.

Photoelectrochemical studies

At first, photoelectrochemical measurements were carried out in an argon-saturated 0.1 M Na_2SO_4 aqueous solution containing 50 mM triethanolamine (TEA) acting as an electron sacrificer using **C_{60}–H_2P**/Au as the working electrode, a platinum counter electrode, and an Ag/AgCl (sat. KCl) reference electrode (hereafter denoted as the Au/**C_{60}–H_2P**/TEA/Pt cell, where/denotes an interface). A stable anodic photocurrent from the electrolyte to the Au electrode appeared immediately upon irradiation of the Au electrode with λ = 428.8 ± 3.9 nm light with a power density of 1.0 mW cm^{-2} at an applied potential of +0.60 V *vs.* Ag/AgCl (sat. KCl) as shown in Fig. 4. The photocurrent fell down instantly when the illumination was cut off. There is a good linear relationship between the photocurrent intensity and the light intensity at each wavelength (from 0.1 to 6.0 mW cm^{-2}). In the absence of TEA, the anodic photocurrent was negligible under otherwise the same experimental conditions. Further addition of TEA (>50 mM) into the electrolyte solution did not increase the photocurrent. The anodic photocurrent increases monotonically with increasing positive bias to the Au electrode (from −0.40 to +0.70 V *vs.* Ag/AgCl (sat. KCl)), whereas the dark current remains constant, as shown in Fig. 5a. The agreement of the action spectrum (Fig. 2b) with the absorption spectrum of **C_{60}–H_2P**/Au (Fig. 2a) in 380–550 nm demonstrates clearly that the porphyrin is the photoactive species responsible for the photocurrent generation. These results demonstrate that photocurrent flows from the electrolyte to the gold electrode *via* the excited states of the porphyrin in the SAM.

Similar photoelectrochemical behavior was observed for the corresponding porphyrin SAMs without the C_{60} on the gold electrode, denoted as the Au/**H_2P**/TEA/Pt cell (Fig. 5a). The quantum yields of photocurrent generation were compared between the Au/**C_{60}–H_2P**/TEA/Pt and Au/**H_2P**/TEA/Pt cells under otherwise the same experimental conditions [applied potential of +0.70 V *vs.* Ag/AgCl (sat. KCl)]. The quantum yields (ϕ) based on the number of photons absorbed by

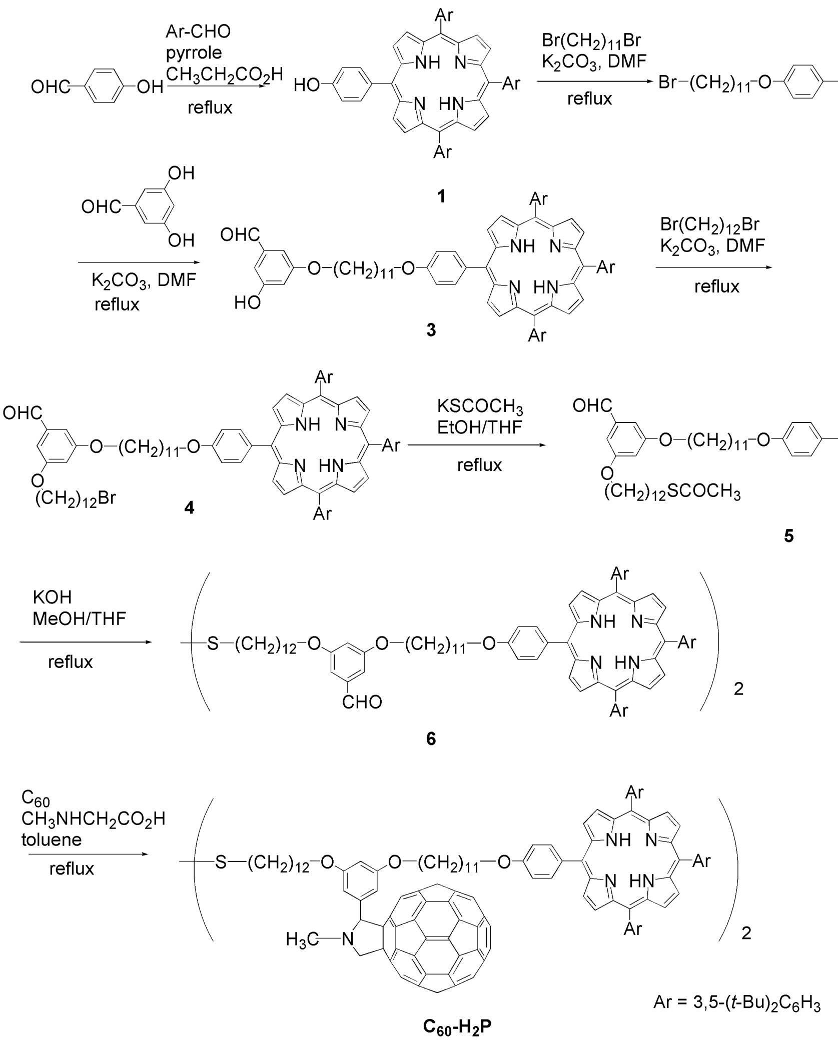

Scheme 1

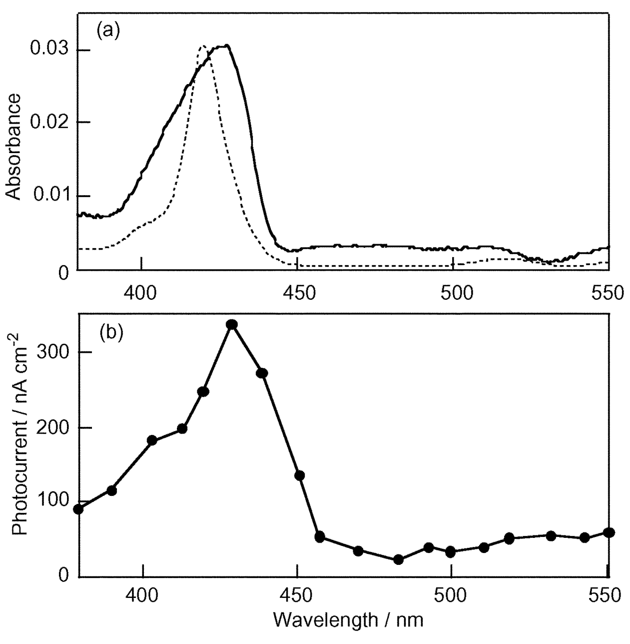

Fig. 2 (a) UV-visible absorption spectra of **C_{60}–H_2P**/Au (solid line) and **C_{60}–H_2P** in THF (dotted line). The spectra are normalized at the Soret band for comparison. (b) Action spectrum of Au/**C_{60}–H_2P**/TEA/Pt cell; input power: 1.0 mW cm^{-2}; applied potential: +0.60 V *vs.* Ag/AgCl (sat. KCl); an argon-saturated 0.1 M Na_2SO_4 aqueous solution containing 50 mM TEA.

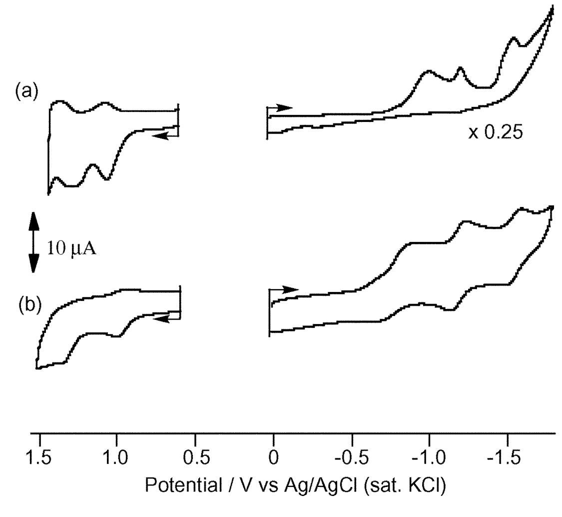

Fig. 3 Cyclic voltammograms of (a) **C_{60}–H_2P**/Au and (b) **C_{60}–H_2P** in CH_2Cl_2 containing 0.2 M *n*-Bu_4NPF_6 with a sweep rate of 0.10 V s^{-1}; electrode area: 0.48 cm^2; counter electrode: Pt wire; reference electrode: Ag/AgCl (sat. KCl).

C_{60}–H_2P on **C_{60}–H_2P**/Au and **H_2P** on **H_2P**/Au were calculated using the input power (λ = 428.8 ± 3.9 nm light of 1.0 mW cm^{-2}), the photocurrent density (*i*), and the absorbance (*A*) on the electrodes (Au/**C_{60}–H_2P**/TEA/Pt cell: i = 662 nA cm^{-2}, A = 0.030; Au/**H_2P**/TEA/Pt cell: i = 32 nA cm^{-2},

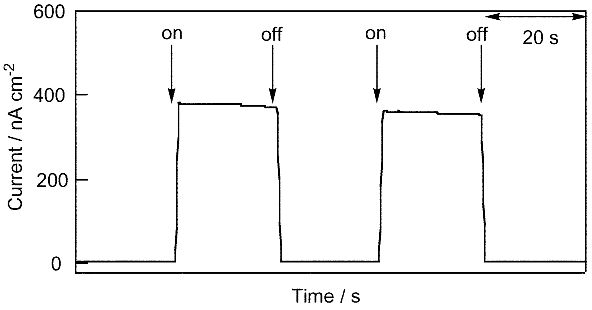

Fig. 4 Photoelectrochemical response of Au/**C_{60}–H_2P**/TEA/Pt cell. Applied potential: +0.60 V *vs.* Ag/AgCl (sat. KCl). λ = 428.8 ± 3.9 nm (1.0 mW cm^{-2}); an argon-saturated 0.1 M Na_2SO_4 aqueous solution containing 50 mM TEA.

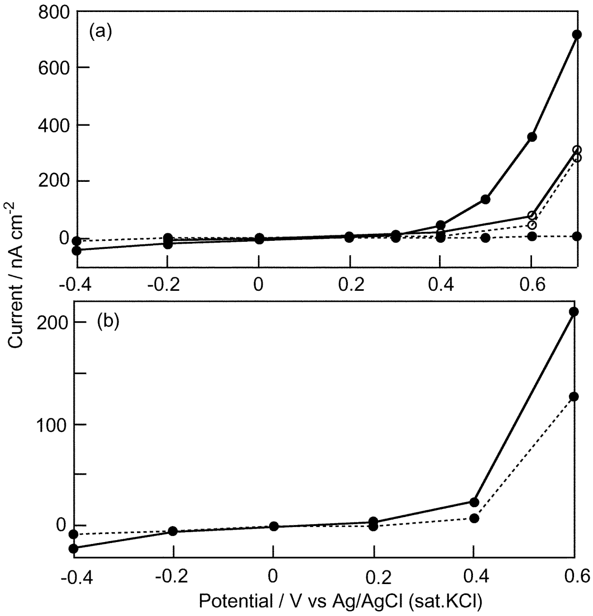

Fig. 5 Photocurrent *vs.* applied potential curves for (a) Au/**C_{60}–H_2P**/TEA/Pt cell (solid line with closed circles) and Au/**H_2P**/TEA/Pt cell (solid line with open circles) and (b) Au/**C_{60}–H_2P**/AsA/Pt cell (solid line with closed circles). The dark currents are shown for comparison [Au/**C_{60}–H_2P**/TEA/Pt cell (dotted line with closed circles); Au/**H_2P**/TEA/Pt cell (dotted line with open circles); Au/**C_{60}–H_2P**/AsA/Pt cell (dotted line with closed circles)]. λ = 428.8 ± 3.9 nm (1.0 mW cm^{-2}); an argon-saturated 0.1 M Na_2SO_4 aqueous solution containing 50 mM TEA or AsA.

A = 0.034). The results are summarized in Table 1. The ϕ value (2.1%) of Au/**C_{60}–H_2P**/TEA/Pt cell is *ca.* 30 times larger than the ϕ value (0.09%) of Au/**H_2P**/TEA/Pt cell. This indicates that the C_{60} moiety mediates ET efficiently from the porphyrin to the gold electrode (*vide infra*).[24]

The effects of other electron donors (*i.e.*, AsA and EDTA) on the photocurrent generation were also examined using the photoelectrochemical cells denoted as Au/**C_{60}–H_2P**/AsA/Pt and Au/**C_{60}–H_2P**/EDTA/Pt, respectively. In the case of the Au/**C_{60}–H_2P**/AsA/Pt cell, the anodic photocurrent increases monotonically with increasing positive bias to the Au electrode [from −0.40 to +0.60 V *vs.* Ag/AgCl (sat. KCl)], whereas the dark current remains constant from −0.4 to +0.4 V *vs.* Ag/AgCl (sat. KCl) and then increased drastically [> +0.4 V *vs.* Ag/AgCl (sat. KCl)]. A similar photoelectrochemical behavior was observed for the Au/**C_{60}–H_2P**/EDTA/Pt cell. The quantum yields of photocurrent generation were compared for the three cells (Au/**C_{60}–H_2P**/TEA or AsA or EDTA/Pt cells), under otherwise the same experimental conditions (applied potential of +0.60 V *vs.* Ag/AgCl (sat. KCl)). The quantum yields of the Au/**C_{60}–H_2P**/TEA/Pt, Au/**C_{60}–H_2P**/AsA/Pt, and Au/**C_{60}–H_2P**/EDTA/Pt cells were determined to be 1.1, 0.26, and 0.003%, respectively (Table 1).

Table 1 Quantum yields of photocurrent generation[a]

		Quantum yields (%)[c]	
SAM	Electron donor[b]	0.6 V[d]	0.7 V[d]
C_{60}–H_2P/Au	TEA	1.1	2.1
	AsA	0.26	[e]
	EDTA	0.003	0.004
H_2P/Au	TEA	0.08	0.09

[a] λ = 428.8 ± 3.9 nm (1.0 mW cm^{-2}), an argon-saturated 0.1 M Na_2SO_4 aqueous solution. [b] 50 mM. [c] Obtained in the standard three electrode systems. The quantum yields of the photocurrent generation were obtained by the following equation: $\phi = (i/e)/[I(1 - 10^{-A})]$ where, $I = (W\lambda)/(hc)$, i is the photocurrent density, e is the elementary charge, I is number of photons per unit area and unit time, λ is the wavelength of light irradiation, A is absorbance of the adsorbed dyes at λ nm, W is light power irradiated at λ nm, c is the light velocity, and h is the Planck constant. [d] Applied potential *vs.* Ag/AgCl (sat. KCl). [e] Not measured.

Mechanism of photocurrent generation

Taking into account the above results together with the well-established photodynamics of porphyrin–fullerene linked systems on electrodes,[18] the mechanism of enhanced photocurrent generation in the Au/**C_{60}–H_2P**/TEA/Pt cell relative to the Au/**H_2P**/TEA/Pt cell is summarized as shown in Scheme 2. The intermolecular ET rate from TEA [TEA/TEA$^{\bullet+}$ = 0.61 V *vs.* Ag/AgCl (sat. KCl)][11d] to the porphyrin excited singlet state [$^1H_2P^*/H_2P^{\bullet-}$ = 0.62 V *vs.* Ag/AgCl (sat. KCl)] is estimated as ~5 × 10^8 s^{-1} at the concentration of TEA (50 mM), assuming the photoinduced ET rate constant is diffusion-limited (~10^{10} M^{-1} s^{-1}). In contrast, the intramolecular ET rate constant from the porphyrin excited singlet state to the C_{60} moiety is estimated as 1.2 × 10^5 s^{-1}, using the Marcus theory of electron transfer.[25,26] The latter ET rate is much slower than the former value. This clearly demonstrates that the initial step is due to intermolecular quenching of the porphyrin excited singlet state by TEA. The porphyrin excited triplet state [$^3H_2P^*/H_2P^{\bullet-}$ = 0.22 V *vs.* Ag/AgCl (sat. KCl)] is not involved in the photocurrent generation because of the endergonic ET from TEA. This process is followed by intramolecular ET from the resulting $H_2P^{\bullet-}$ [$H_2P^{\bullet-}/H_2P$ = −1.28 V *vs.* Ag/AgCl (sat. KCl)][27] to C_{60} [$C_{60}/C_{60}^{\bullet-}$ = −0.62 V *vs.* Ag/AgCl (sat. KCl)],[18c] and then $C_{60}^{\bullet-}$ to the gold electrode, to generate the anodic photocurrent. Since the intermolecular ET process from EDTA [EDTA/EDTA$^{\bullet+}$ = 1.26 V *vs.* Ag/AgCl (sat. KCl)] to the porphyrin excited singlet state is endergonic, the quantum yield of the photocurrent generation for the Au/**C_{60}–H_2P**/EDTA/Pt cell (0.003 %) is negligible as compared to that of the Au/**C_{60}–H_2P**/TEA/Pt cell (1.1%).

Although the ET process from AsA [−0.19 V *vs.* Ag/AgCl (sat. KCl)][4] to the porphyrin excited singlet state is more

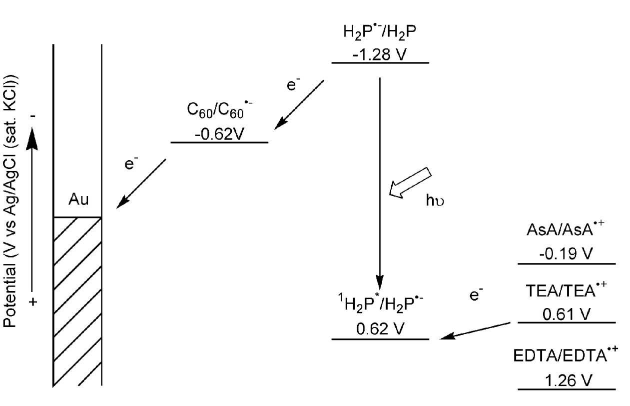

Scheme 2

exergonic than that from TEA, the quantum yield of photocurrent generation for the Au/**C_{60}–H_2P**/AsA/Pt cell (0.26%) is even lower than that of the Au/**C_{60}–H_2P**/TEA/Pt cell (1.1%). In the case of the Au/**C_{60}–H_2P**/TEA/Pt cell, the resulting $TEA^{\bullet+}$ is rearranged to its reduced form by H atom abstraction from another TEA.[28] Such an irreversible transformation of $TEA^{\bullet+}$ prevents the back electron transfer from $H_2P^{\bullet-}$ to $TEA^{\bullet+}$, resulting in efficient photocurrent generation as compared to the case of AsA which does not undergo irreversible decomposition after intermolecular ET to the porphyrin excited singlet state.

We have already reported a series of C_{60} SAM cells on gold electrodes, where the C_{60} and the gold surface are linked with a similar methylene spacer.[4] When the modified gold electrodes were irradiated at $\lambda = 403.0 \pm 6.9$ nm, the quantum yields of the photocurrent generation in the presence of 50 mM AsA at a bias of 0.10 V (*vs.* Ag/AgCl (sat. KCl)) were determined as 7.5 to 9.8%, which is about 4 times higher than the present system. The anodic photocurrent generation can be explained as follows: the generation of vectorial electron flow from the electron sacrificer to the gold electrode *via* the excited triplet state of the C_{60}. The high quantum yields of the C_{60} SAM cells relative to the present system can be ascribed to the efficient electron injection from the resulting C_{60} radical anion to the gold electrode. In contrast, the competition between a slow charge-shift reaction from the resulting porphyrin radical anion to the C_{60} and the energy-wasting back ET is responsible for the relatively poor photocurrent generation in the present system. We have also prepared the ferrocene–porphyrin–C_{60} SAMs on a gold electrode and the photoelectrochemical properties were examined in the presence of methyl viologen (MV^{2+}) and oxygen as electron acceptors.[18c] When the modified gold electrodes were irradiated at 438.5 ± 4.9 nm, the quantum yields were 20 to 25% at a bias of −0.20 V (*vs.* Ag/AgCl (sat. KCl)). Multistep ET from the porphyrin singlet excited state to the C_{60} followed by charge-shift from the ferrocene to the resulting porphyrin radical cation results in the efficient formation of the charge-separated state (ferrocene$^{\bullet+}$–porphyrin-$C_{60}^{\bullet-}$) with a long lifetime on the gold electrode. This leads to the cathodic photocurrent generation, which is in sharp contrast with the present system.

Conclusion

Self-assembled monolayers of fullerene–porphyrin linked dyads on a gold electrode have been prepared to exhibit anodic photocurrent generation for the first time. The spectroscopic and electrochemical studies reveal the well-packed structure of the fullerene–porphyrin dyad molecules on the gold electrode. The efficiency of photocurrent generation is much improved as compared to the porphyrin reference system without the C_{60} moiety. These results clearly show that C_{60} is a good electron mediator between the porphyrin moiety and the gold electrode.

Experimental

General

^{1}H-NMR spectra were measured on a JEOL EX-270 spectrometer. Time of flight (TOF) mass spectra (MS) were measured on an Applied Biosystems Voyger RP, with dithranol as a matrix. UV-visible spectra were obtained on a Shimadzu UV-3100 spectrometer.

Materials

Gold electrodes for photoelectrochemical measurements (roughness factor (R) = 1.1) were prepared by a vacuum deposition technique with titanium (5–10 nm) and gold (20–100 nm) in sequence onto a Si(100) wafer whereas gold (20 nm) was evaporated onto mica (R = 1.1) for electrochemical measurements and onto transparent glass slides (R = 1.5) for UV-visible absorption measurements.[8c] Roughness factors were estimated by iodine chemisorption on a Au(111) surface.[8c] All solvents and chemicals were of reagent grade quality, purchased commercially and used without further purification unless otherwise noted. Tetrabutylammonium hexafluorophosphate used as a supporting electrolyte for the electrochemical measurements was obtained from Tokyo Kasei Organic Chemicals and recrystallized from methanol. Dry toluene and dry methylene chloride were heated at reflux and distilled from CaH_2 prior to use. Thin-layer chromatography and flash column chromatography were performed with Alt. 5554 DC-Alufolien Kieselgel 60 F_{254} (Merck) and Fujisilica BW300, respectively.

Porphyrin 1

3,5-Di-*tert*-butylbenzaldehyde[19] (21.36 g. 97.8 mmol) and 4-hydroxybenzaldehyde (5.98 g, 49.0 mmol) were dissolved in propionic acid (1 L) and warmed up to reflux.[20] Then pyrrole (10.2 mL, 147 mmol) was added and the reflux was continued for 1 h. After cooling the mixture the solvent was removed under reduced pressure. The residue was purified by flash column chromatography 3 times (benzene), and the second red band (R_f value = 0.35 (benzene)) gave the desired porphyrin **1** as a red solid (2.35 g, 2.43 mmol, 6.6%). ^{1}H NMR (270 MHz, $CDCl_3$) δ = 8.89 (s, 4H), 8.87 (s, 4H), 8.08 (m, 8H), 7.79 (t, J = 2 Hz, 3H), 7.19 (d, J = 8 Hz, 2H), 1.52 (s, 54H), −2.71 (br s, 2H).

Porphyrin 2

Porphyrin **1** (483 mg, 0.5 mmol), 1,11-dibromoundecane (1.57 g, 5.00 mmol), and potassium carbonate anhydrous (690 mg, 5.00 mmol) were dissolved in DMF (40 mL) and the mixture was warmed up to reflux for 2 h. After cooling the solvent was removed under reduced pressure. The residue was purified by flash column chromatography (hexane : benzene = 1 : 1; R_f value = 0.9 (hexane : benzene = 1 : 1)) and the reprecipitation from benzene–methanol gave the desired porphyrin **2** (347 mg, 0.289 mmol, 58%). ^{1}H NMR (270 MHz, $CDCl_3$) δ = 8.89 (s, 4H), 8.87 (s, 4H), 8.12 (d, J = 8 Hz, 2H), 8.08 (d, J = 2 Hz, 4H), 8.07 (d, J = 2 Hz, 2H), 7.78 (m, 3H), 7.26 (d, J = 8 Hz, 2H), 4.25 (t, J = 7 Hz, 2H), 3.43 (t, J = 7 Hz, 2H), 1.99 (quintet, J = 7 Hz, 2H), 1.87 (quintet, J = 7 Hz, 2H), 1.7–1.2 (m, 68H), −2.70 (br s, 2H).

Porphyrin 3

Porphyrin **2** (240 mg, 0.200 mmol), 3,5-dihydroxybenzaldehyde (552 mg, 4.00 mmol), and potassium carbonate anhydrous (552 mg, 4.00 mmol) were dissolved in DMF (40 mL) and the mixture was warmed up to reflux for 4 h. After cooling the solvent was removed under reduced pressure. The purification by flash column chromatography (ethyl acetate : benzene = 1 : 19; R_f value = 0.1 (benzene)) and the reprecipitation from benzene–methanol gave the desired porphyrin **3** (106 mg, 84.3 μmol, 42%). ^{1}H NMR (270 MHz, $CDCl_3$) δ = 9.78 (s, 1H), 8.89 (s, 4H), 8.87 (s, 4H), 8.12 (d, J = 8 Hz, 2H), 8.08 (m, 6H), 7.78 (t, J = 2 Hz, 3H), 7.27 (d, J = 8 Hz, 2H), 6.94 (dd, J = 2 and 2 Hz, 1H), 6.71 (dd, J = 2 and 2 Hz, 1H), 6.47 (t, 1H, J = 2 Hz), 4.26 (t, J = 7 Hz, 2H), 3.95 (t, J = 7 Hz, 2H), 1.99 (quintet, J = 7 Hz, 2H), 1.78 (quintet, J = 7 Hz, 2H), 1.7–1.2 (m, 68H).

Porphyrin 4

Porphyrin **3** (86.2 mg, 68.5 μmol), 1,12-dibromododecane (450 mg, 1.37 mmol), and potassium carbonate anhydrous (189 mg, 1.37 mmol) were dissolved in DMF (30 mL) and the mixture was warmed up to reflux for 1 h. After cooling the solvent was removed under reduced pressure. The purification by flash column chromatography (benzene; R_f value = 0.9 (benzene)) and the reprecipitation from benzene–methanol gave the desired porphyrin **4** (59.2 mg, 39.3 μmol, 57 %). ^{1}H NMR (270 MHz, $CDCl_3$) δ = 9.88 (s, 1H), 8.89 (s, 4H), 8.87 (s, 4H), 8.12 (d, J = 8 Hz, 2H), 8.08 (s, 6H), 7.78 (s, 3H), 7.27 (d, J = 8 Hz, 2H), 6.98 (s, 2H), 6.70 (s, 1H), 4.25 (t, J = 7 Hz, 2H), 4.00 (t, J = 7 Hz, 2H), 3.97 (t, J = 7 Hz, 2H), 3.39 (t, J = 7 Hz, 2H), 1.99 (quintet, J = 7 Hz, 2H), 1.80 (m, 6H), 1.7–1.2 (m, 84H), −2.70 (br s, 2H).

Porphyrin 5

Porphyrin **4** (60.0 mg, 39.9 μmol) and potassium thioacetate (19.4 mg, 0.170 mmol) were dissolved in a mixture of THF and ethanol (15 mL : 15 mL) and warmed up to reflux for 2 h. After cooling the solvent was removed under reduced pressure. The purification by flash column chromatography (hexane : benzene (1 : 1), hexane : benzene (1 : 2), then benzene; R_f value = 0.7 (benzene)) and the reprecipitation from benzene–methanol gave the desired porphyrin **5** (33.7 mg, 22.5 μmol, 56%). ^{1}H NMR (270 MHz, $CDCl_3$) δ = 9.87 (s, 1H), 8.89 (s, 4H), 8.88 (s, 4H), 8.12 (d, J = 8 Hz, 2H), 8.08 (s, 6H), 7.78 (s, 3H), 7.27 (d, J = 8 Hz, 2H), 6.98 (s, 2H), 6.70 (s, 1H), 4.24 (t, J = 7 Hz, 2H), 4.00 (t, J = 7 Hz, 2H), 3.97 (t, J = 7 Hz, 2H), 2.84 (t, J = 7 Hz, 2H), 2.30 (s, 3H), 1.99 (quintet, J = 7 Hz, 2H), 1.79 (m, 4H), 1.7–1.2 (m, 86H), −2.69 (br s, 2H).

Porphyrin 6

Porphyrin **5** (33.7 mg, 22.5 μmol) and KOH (40 mg, 1 mmol) were suspended in a mixture of THF and ethanol (20 mL : 20 mL) and nitrogen gas was bubbled through it for 30 min. Then the suspension was warmed up to reflux for 5 min. After cooling the solvent was removed under reduced pressure. The purification by flash column chromatography (benzene; R_f value = 0.6 (benzene)) and the reprecipitation from benzene–methanol gave the desired porphyrin **6** (26.5 mg, 9.09 μmol, 81%). ^{1}H NMR (270 MHz, $CDCl_3$) δ = 9.86 (s, 2H), 8.89 (s, 8H), 8.88 (s, 8H), 8.12 (d, J = 8 Hz, 4H), 8.08 (s, 12H), 7.78 (s, 6H), 7.27 (d, J = 8 Hz, 4H), 6.97 (s, 4H), 6.69 (s, 2H), 4.24 (t, J = 7 Hz, 4H), 3.99 (t, J = 7 Hz, 4H), 3.96 (t, J = 7 Hz, 4H), 2.65 (t, J = 7 Hz, 4H), 1.98 (quintet, J = 7 Hz, 4H), 1.78 (m, 8H), 1.7–1.2 (m, 172H), −2.69 (br s, 4H).

C_{60}–H_2P

Porphyrin **6** (26.5 mg, 9.09 μmol), C_{60} (42 mg, 3 eq.), and *N*-methylglycine (52 mg, 30 eq.) were dissolved in toluene (30 mL) and nitrogen gas was bubbled through it for 30 min.[21] Then the mixture was warmed up to reflux for 13 h. After cooling the solvent was removed under reduced pressure. The purification by flash column chromatography (hexane : benzene (1 : 1), then benzene; R_f value = 0.35 (hexane : benzene (1 : 1)) and the reprecipitation from benzene–methanol gave the desired porphyrin–fullerene dimer **C_{60}–H_2P** (23.4 mg, 5.31 μmol, 58%). ^{1}H NMR (270 MHz, $CDCl_3$) δ = 8.88 (s, 16H), 8.07 (s, 16H), 7.78 (s, 6H), 7.27 (d, J = 8 Hz, 4H), 6.86 (br s, 4H), 6.35 (s, 2H), 4.57 (d, J = 7 Hz, 2H), 4.47 (s, 2H), 4.27 (br s, 4H), 3.88 (br s, 10H), 2.70 (s, 6H), 2.64 (t, J = 7 Hz, 4H), 1.97 (br s, 4H), 1.7–1.2 (m, 180H), −2.71 (br s, 4H); MS (FAB) 4410 (M + H^+).

Acknowledgement

This work has been carried out at the Strategic Research Base "Handai Frontier Research Center" supported by the Japanese Government's Special Coordination Fund for Promoting Science and Technology. This work was supported by a Grant-in-Aid for Scientific Research and a Grant-in-Aid for the Development of Innovative Technology (No. 12310) from The Ministry of Education, Culture, Sports, Science and Technology, Japan.

References

1 (*a*) A. Ulman, *An Introduction to Ultrathin Organic Films*, Academic Press, San Diego, 1991; (*b*) *Molecular Electronics*, ed. J. Jortner and M. Ratner, Blackwell Science, Oxford, 1997; (*c*) C. A. Mirkin, *Inorg. Chem.*, 2000, **39**, 2258; (*d*) A. N. Shipway, E. Katz and I. Willner, *ChemPhysChem.*, 2000, **1**, 18.

2 (*a*) C. A. Mirkin and W. B. Caldwell, *Tetrahedron*, 1996, **52**, 5113; (*b*) X. Shi, W. B. Caldwell, K. Chen and C. A. Mirkin, *J. Am. Chem. Soc.*, 1994, **116**, 11598; (*c*) W. B. Caldwell, K. Chen, C. A. Mirkin and S. J. Babinec, *Langmuir*, 1993, **9**, 1945; (*d*) Y.-S. Shon, K. F. Kelly, N. J. Halas and T. R. Lee, *Langmuir*, 1999, **15**, 5329.

3 (*a*) F. Arias, L. A. Godínez, S. R. Wilson, A. E. Kaifer and L. Echegoyen, *J. Am. Chem. Soc.*, 1996, **118**, 6086; (*b*) O. Domínguez, L. Echegoyen, F. Cunha and N. Tao, *Langmuir*, 1998, **14**, 821; (*c*) L. Echegoyen and L. E. Echegoyen, *Acc. Chem. Res.*, 1998, **31**, 593; (*d*) T. Hatano, A. Ikeda, T. Akiyama, S. Yamada, M. Sano, Y. Kanekiyo and S. Shinkai, *J. Chem. Soc., Perkin Trans. 2*, 2000, 909; (*e*) S.-G. Liu, C. Martineau, J.-M. Raimundo, J. Roncali and L. Echegoyen, *Chem. Commun.*, 2001, 913.

4 H. Imahori, T. Azuma, A. Ajavakom, H. Norieda, H. Yamada and Y. Sakata, *J. Phys. Chem. B*, 1999, **103**, 7233.

5 (*a*) M. Lahav, T. Gabriel, A. N. Shipway and I. Willner, *J. Am. Chem. Soc.*, 1999, **121**, 258; (*b*) M. Lahav, V. Heleg-Shabtai, J. Wasserman, E. Katz, I. Willner, H. Dürr, Y.-Z. Hu and S. H. Bossmann, *J. Am. Chem., Soc.*, 2000, **122**, 11480; (*c*) K. Uosaki, T. Kondo, X.-Q. Zhang and M. Yanagida, *J. Am. Chem. Soc.*, 1997, **119**, 8367; (*d*) T. Kondo, M. Yanagida, S.-i. Nomura, T. Ito and K. Uosaki, *J. Electroanal. Chem.*, 1997, **438**, 121.

6 (*a*) E. Katz and I. Willner, *Langmuir*, 1997, **13**, 3364; (*b*) J. Zak, H. Yuan, M. Ho, L. K. Woo and M. D. Porter, *Langmuir*, 1993, **9**, 2772; (*c*) J. E. Hutchison, T. A. Postlethwaite and R. W. Murray, *Langmuir*, 1993, **9**, 3277; (*d*) T. R. E. Simpson, D. J. Revell, M. J. Cook and D. A. Russell, *Langmuir*, 1997, **13**, 460; (*e*) D. T. Gryko, F. Zhao, A. A. Yasseri, K. M. Roth, D. F. Bocian, W. G. Kuhr and J. S. Lindsey, *J. Org. Chem.*, 2000, **65**, 7356.

7 (*a*) T. Yamada, T. Hashimoto, S. Kikushima, T. Ohtsuka and M. Nango, *Langmuir*, 2001, **17**, 4634; (*b*) N. Kanayama, T. Kanbara and H. Kitano, *J. Phys. Chem. B*, 2000, **104**, 271; (*c*) D. A. Offord, S. B. Sachs, M. S. Ennis, T. A. Eberspacher, J. H. Griffin, C. E. D. Chidsey and J. P. Collman, *J. Am. Chem. Soc.*, 1998, **120**, 4478; (*d*) W. Han, S. Li, S. M. Lindsay, D. Gust, T. A. Moore and A. L. Moore, *Langmuir*, 1996, **12**, 5742; (*e*) D. L. Pilloud, X. Chen, P. L. Dutton and C. C. Moser, *J. Phys. Chem. B*, 2000, **104**, 2868.

8 (*a*) S. Fukuzumi and H. Imahori, in *Electron Transfer in Chemistry*, Vol. 2, ed. V. Balzani, Wiley-VCH, Weinheim, 2001, p. 927; (*b*) H. Imahori, H. Norieda, S. Ozawa, K. Ushida, H. Yamada, T. Azuma, K. Tamaki and Y. Sakata, *Langmuir*, 1998, **14**, 5335; (*c*) H. Imahori, H. Norieda, Y. Nishimura, I. Yamazaki, K. Higuchi, N. Kato, T. Motohiro, H. Yamada, K. Tamaki, M. Arimura and Y. Sakata, *J. Phys. Chem. B*, 2000, **104**, 1253; (*d*) H. Imahori, T. Hasobe, H. Yamada, Y. Nishimura, I. Yamazaki and S. Fukuzumi, *Langmuir*, 2001, **17**, 4925.

9 (*a*) J. J. Hickman, D. Ofer, C. Zou, M. S. Wrighton, P. E. Laibinis and G. M. Whitesides, *J. Am. Chem. Soc.*, 1991, **113**, 1128; (*b*) C. D. Frisbie, J. R. Martin, R. R. Duff, Jr and M. S. Wrighton, *J. Am. Chem. Soc.*, 1992, **114**, 7142; (*c*) S. Creager, C. J. Yu, C. Bambad, S. O'Connor, T. MacLean, E. Lam, Y. Chong, G. T. Olsen, J. Luo, M. Gozin and J. F. Kayyem, *J. Am. Chem. Soc.*, 1999, **121**, 1059; (*d*) T. Kondo, S. Horiuchi, I. Yagi, S. Ye and K. Uosaki, *J. Am. Chem. Soc.*, 1999, **121**, 391; (*e*) A. Hatzor, T. Moav, H. Cohen, S. Matlis, J. Libman, A. Vaskevich, A. Shanzer and I. Rubinstein, *J. Am. Chem. Soc.*, 1998, **120**, 13469.

10 (*a*) W. B. Caldwell, D. J. Campbell, K. Chen, B. R. Herr, C. A. Mirkin, A. Malik, M. K. Durbin, P. Dutta and K. G. Huang, *J. Am. Chem. Soc.*, 1995, **117**, 6071; (*b*) D. J. Campbell, B. R. Herr, J. C. Hulteen, R. P. Van Duyne and C. A. Mirkin, *J. Am. Chem. Soc.*, 1996, **118**, 10211; (*c*) D. G. Walter, D. J. Campbell and C. A. Mirkin, *J. Phys. Chem. B*, 1999, **103**, 402.

11 (*a*) I. Willner, *Acc. Chem. Res.*, 1997, **30**, 347; (*b*) R. Blonder, S. Levi, G. Tao, I. Ben-Dov and I. Willner, *J. Am. Chem. Soc.*, 1997, **119**, 10467; (*c*) A. Doron, M. Portnoy, M. Lion-Dagan, E. Katz and I. Willner, *J. Am. Chem. Soc.*, 1996, **118**, 8937; (*d*) T. Morita, S. Kimura, S. Kobayashi and Y. Imanishi, *J. Am. Chem. Soc.*, 2000, **122**, 2850; (*e*) Y. Koide, N. Terasaki, T. Akiyama and S. Yamada, *Thin Solid Films*, 1999, **350**, 223.

12 (*a*) M. A. Fox, *Acc. Chem. Res.*, 1999, **32**, 201; (*b*) M. O. Wolf and M. A. Fox, *J. Am. Chem. Soc.*, 1995, **117**, 1845; (*c*) W. Li, V. Lynch, H. Thompson and M. A. Fox, *J. Am. Chem. Soc.*, 1997, **119**, 7211; (*d*) S. Reese and M. A. Fox, *J. Phys. Chem. B*, 1998, **102**, 9820.

13 (*a*) N. Martín, L. Sánchez, B. Illescas and I. Pérez, *Chem. Rev.*, 1998, **98**, 2527; (*b*) M. Prato, *J. Mater. Chem.*, 1997, **7**, 1097; (*c*) F. Diederich and M. Gómez-López, *Chem. Soc. Rev.*, 1999, **28**, 263; (*d*) D. Gust, T. A. Moore and A. L. Moore, *Acc. Chem. Res.*, 2001, **34**, 40; (*e*) A. W. Jensen, S. R. Wilson and D. I. Schuster, *Bioorg. Med. Chem.*, 1996, **4**, 767.

14 (*a*) H. Imahori and Y. Sakata, *Adv. Mater.*, 1997, **9**, 537; (*b*) H. Imahori and Y. Sakata, *Eur. J. Org. Chem.*, 1999, 2445; (*c*) D. M. Guldi, *Chem. Commun.*, 2000, 321; (*d*) D. M. Guldi and M. Prato, *Acc. Chem. Res.*, 2000, **33**, 695.

15 (*a*) H. Imahori, K. Hagiwara, T. Akiyama, M. Aoki, S. Taniguchi, T. Okada, M. Shirakawa and Y. Sakata, *Chem. Phys. Lett.*, 1996, **263**, 545; (*b*) H. Imahori, K. Tamaki, H. Yamada, K. Yamada, Y. Sakata, Y. Nishimura, I. Yamazaki, M. Fujitsuka and O. Ito, *Carbon*, 2000, **38**, 1599; (*c*) H. Imahori, N. V. Tkachenko, V. Vehmanen, K. Tamaki, H. Lemmetyinen, Y. Sakata and S. Fukuzumi, *J. Phys. Chem. A*, 2001, **105**, 1750; (*d*) V. Vehmanen, N. V. Tkachenko, H. Imahori, S. Fukuzumi and H. Lemmetyinen, *Spectrochim. Acta, Part A*, 2001, **57**, 2229.

16 D. M. Guldi and K.-D. Asmus, *J. Am. Chem. Soc.*, 1997, **119**, 5744.

17 (*a*) H. Imahori, K. Hagiwara, T. Akiyama, S. Taniguchi, T. Okada and Y. Sakata, *Chem. Lett.*, 1995, 265; (*b*) H. Imahori, K. Hagiwara, M. Aoki, T. Akiyama, S. Taniguchi, T. Okada, M. Shirakawa and Y. Sakata, *J. Am. Chem. Soc.*, 1996, **118**, 11771; (*c*) C. Luo, D. M. Guldi, H. Imahori, K. Tamaki and Y. Sakata, *J. Am. Chem. Soc.*, 2000, **122**, 6535; (*d*) H. Imahori, K. Tamaki, D. M. Guldi, C. Luo, M. Fujitsuka, O. Ito, Y. Sakata and S. Fukuzumi, *J. Am. Chem. Soc.*, 2001, **123**, 2607; (*e*) H. Imahori, D. M. Guldi, K. Tamaki, Y. Yoshida, C. Luo, Y. Sakata and S. Fukuzumi, *J. Am. Chem. Soc.*, 2001, **123**, 6617.

18 (*a*) T. Akiyama, H. Imahori, A. Ajavakom and Y. Sakata, *Chem. Lett.*, 1996, 907; (*b*) H. Imahori, S. Ozawa, K. Ushida, M. Takahashi, T. Azuma, A. Ajavakom, T. Akiyama, M. Hasegawa, S. Taniguchi, T. Okada and Y. Sakata, *Bull. Chem. Soc. Jpn.*, 1999, **72**, 485; (*c*) H. Imahori, H. Yamada, Y. Nishimura, I. Yamazaki and Y. Sakata, *J. Phys. Chem. B*, 2000, **104**, 2099; (*d*) H. Imahori, H. Norieda, H. Yamada, Y. Nishimura, I. Yamazaki, Y. Sakata and S. Fukuzumi, *J. Am. Chem. Soc.*, 2001, **123**, 100; (*e*) H. Imahori and S. Fukuzumi, *Adv. Mater.*, 2001, **13**, 1197.

19 M. S. Newman and L. F. Lee, *J. Org. Chem.*, 1972, **37**, 4468.

20 A. D. Adler, F. R. Longo, J. D. Finarelli, J. Goldmacher, J. Assour and L. Korsakoff, *J. Org. Chem.*, 1967, **32**, 476.

21 (*a*) M. Maggini, G. Scorrano and M. Prato, *J. Am. Chem. Soc.*, 1993, **115**, 9798; (*b*) M. Prato and M. Maggini, *Acc. Chem. Res.*, 1998, **31**, 519.

22 The red-shift and broadening of $\mathbf{H_2P}$/Au were reported to be due to the partially stacked side-by-side porphyrin aggregation in the SAM,[8c] see: R. F. Khairutdinov and N. Serpone, *J. Phys. Chem. B*, 1999, **103**, 761.

23 The adsorbed amounts of $\mathbf{C_{60}}$–$\mathbf{H_2P}$ and ferrocene–porphyrin–$\mathbf{C_{60}}$ may be controlled by the size of the C_{60} moiety when these molecules are well-packed on the gold surfaces.

24 The chain length effect of photocurrent generation using the gold electrode modified with the same porphyrin including $\mathbf{H_2P}$/Au has already been reported.[8c] The quantum yield for the photocurrent generation increases with an increase in the spacer length up to the number of methylenes length, 6, and then it starts decreasing with a further increase in the spacer length. Such a dependence of the quantum yield on the spacer length can be explained by the competition between an electron transfer and an energy transfer quenching of the singlet excited state of the porphyrin to the gold electrode. Thus, the quantum yield of photocurrent generation for the porphyrin reference system where the porphyrin is located at the same position as Au/$\mathbf{C_{60}}$–$\mathbf{H_2P}$/TEA/Pt cell would be rather low as compared to the quantum yield of the Au/$\mathbf{H_2P}$/TEA/Pt cell (0.09%).

25 The following Marcus equation[26] was used to estimate the ET rate constant from $^1H_2P^*$ to C_{60}. $k_{ET} = (4\pi^3/h^2\lambda k_BT)^{1/2}\ V^2 \exp[-(\Delta G_{ET}{}^{o}+\lambda)^2/4\lambda k_BT]$ where, $V^2 = V_0{}^2\exp(-\beta R_{ee})$, $\lambda = \lambda_i + \lambda_s$, and $\lambda_s = e^2(1/(2R_D) + 1/(2R_A) - 1/R_{ee})(1/\varepsilon_s - 1/\varepsilon_{op})$. Total reorganization energy, λ, was estimated as 1.00 eV from the internal reorganization energy λ_i (=0.05 eV)[15d] and the solvent reorganization energy (λ_s), using the λ_s values (0.61 eV and 1.04 eV) of previously reported porphyrin–C_{60} dyads (R_{ee} = 11.9 Å)[17d] and zinc porphyrin–free base porphyrin–C_{60} triads (R_{ee} = 30.3 Å),[17d] respectively, and the edge-to-edge distance (R_{ee} = 22.9 Å) of the H_2P and C_{60} moieties. The electronic coupling matrix element, V, was estimated as 0.22 cm^{-1}, using a decay coefficient, β (=0.60 $Å^{-1}$),[17e] V_0 = 210 cm^{-1},[17e] and the edge-to-edge distance of H_2P and C_{60} (R_{ee} = 22.9 Å). $-\Delta G_{ET}{}^0$ value was estimated as 0.31 eV from the redox potentials of the porphyrin [0.97 V *vs.* Ag/AgCl (sat. KCl)] and the C_{60} [−0.62 V *vs.* Ag/AgCl (sat. KCl)][18c] and the excitation energy (1.90 eV)[17c].

26 R. A. Marcus and N. Sutin, *Biochim. Biophys. Acta*, 1985, **811**, 265.

27 H. Yamada, H. Imahori, Y. Nishimura, I. Yamazaki and S. Fukuzumi, *Chem. Commun.*, 2000, 1921.

28 (*a*) S.-F. Chan, M. Chou, C. Creutz, T. Matsubara and N. Sutin, *J. Am. Chem. Soc.*, 1981, **103**, 369; (*b*) A. J. Downard, N. A. Surridge, S. Gould, T. J. Meyer, A. Deronzier and J.-C. Moutet, *J. Phys. Chem.*, 1990, **94**, 6754; (*c*) S. Matsuoka, K. Yamamoto, T. Ogata, M. Kusaba, N. Nakashima, E. Fujita and S. Yanagida, *J. Am. Chem. Soc.*, 1993, **115**, 601; (*d*) A. Aoki, Y. Abe and T. Miyashita, *Langmuir*, 1999, **15**, 1463.